Available online at www.sciencedirect.com

ScienceDirect

Procedia Engineering 00 (2017) 000–000

Procedia Engineering

www.elsevier.com/locate/procedia

International High- Performance Built Environment Conference – A Sustainable Built Environment Conference 2016 Series (SBE16), iHBE 2016

A methodological framework to assess the thermal performance of green infrastructure through airborne remote sensing

Carlos Bartesaghi Koc[a,b] *, Paul Osmond[a,b], Alan Peters[a], Matthias Irger

[a]*Faculty of Built Environment - UNSW, Sydney NSW 2052, Australia*
[b]*CRC for Low Carbon Living Ltd., Tyree Energy Technologies Building - UNSW, Sydney NSW 2052, Australia*

Abstract

This paper presents a methodological framework for a more accurate assessment of the thermal performance of green infrastructure (GI) using a combination of airborne remote sensing, field measurements and numerical modelling. The proposed framework consists of: (a) controlling intervening variables and classifying sites according to urban morphology, (b) classifying GI according to a newly developed typology, (c) quantifying and allocating a set of indicators/metrics to each typology, and (d) analysing and comparing data spatially and statistically. The proposed framework provides a standardised protocol that urban planners and practitioners can apply to quantify, compare and report the results of microclimate studies.

Peer-review under responsibility of the organizing committee iHBE 2016.

Keywords: Urban heat island; green infrastructure typology; local climate zones; urban microclimate; remote sensing; evapotranspiration.

1. Introduction

It has been demonstrated that an increment of vegetation cover corresponds with a reduction of land surface temperature (LST) and the attenuation of the surface urban heat island (SUHI) [1, 2]. Remote sensing has been commonly employed to investigate the cooling effects of green infrastructure (GI) because large areas can be

* Corresponding author. Tel.: +61 (02) 9385 5023; Mob.: +61 (0) 450 861 020.
E-mail address: c.bartesaghikoc@unsw.edu.au

Peer-review under responsibility of the organizing committee iHBE 2016.

monitored and analysed simultaneously and continuously [1, 3–5]. However, it mainly focuses on surface temperature rather than air temperature, whereas the latter is more related to human thermal comfort [4, 5]. Numerous studies have analysed the influence of spatial patterns, amount of vegetation and impervious surface fractions on LST [6–12] while others have focused on the extent and spatial variability of urban cool islands [13–17] and park cool islands [18–21]. Overall, most previous work has been conducted at city-wide level, and little at very fine scales.

However, there is still little guidance on the most effective composition, amount and arrangement of GI required to provide maximum cooling effects [4, 22]. There is an urgent necessity for tools to inform policy development and support urban planners and designers on the strategic implementation of GI for heat mitigation [2, 4]. This paper responds to this gap and presents a methodological framework for a more precise and comprehensive assessment of the thermal performance of GI at high spatial resolution by integrating airborne remote sensing, ground-based measurements and numerical modelling. This framework draws on the theoretical and methodological approaches of multiple disciplines and builds on previous guidelines published by Coutts et al. [2, 23], Harris et al. [4], and Irger [24]. The purposes of developing this framework are: (a) to identify a list of functional, morphological and configurational indicators/metrics to quantify the cooling effects of GI in a more comprehensive way; (b) to combine empirical observations and predictive methods; and (c) to propose a standardised workflow that makes use of readily accessible data and is replicable by researchers, practitioners and urban planners.

2. Methodology

This paper is based on a systematic literature review of 66 studies (from 2010 onwards) that reported on the cooling effects of GI using remote sensing. Publications were systematically analysed to evaluate current methodologies, identify indicators, and verify the type and quality of data sources and instruments. Relevant information was identified to formulate a new methodological framework to tackle the shortcomings and gaps identified in current research. The selected studies met the following inclusion criteria:

- Studies were peer-reviewed and written in English.
- Studies reported on the thermal benefits of GI by comparing climatological conditions (dependent variables) against measurable characteristics or metrics of GI (independent variables) at different spatial scales.
- Studies used remote sensing solely or in combination with other methods.
- Studies assessed any form of vegetation (green open spaces, trees, green roofs, etc.) and/or water bodies.

3. Overview of recent studies

3.1. Key parameters of investigation

Remotely-sensed studies have investigated the relationships between surface/air temperatures (dependent variables) and independent variables corresponding to functional, morphological and configurational attributes of GI [25]. They have also quantified the magnitude of the contribution of GI-derived variables on dependent variables. These relationships can be influenced by intervening variables derived from either climatological or morphological aspects. Table 1 presents a detailed list of key dependent, independent and intervening variables from the literature.

3.2. Data sources and data acquisition

Remotely sensed thermal infrared (TIR) data has been extensively employed to determine the extent and magnitude of SUHI [4, 5]. Compared to ground-based monitoring, TIR imagery enables a synchronised capture of radiant surface temperatures over large areas [4, 5, 24]. An accurate estimation of LST requires corrections for emissivity and atmospheric effects (upward emission, absorption and downward irradiance) [5]. However, emissivity values vary among surfaces (concrete, roof tiles, grass, and metal) and depend on factors such as roughness, structure, chemical composition or water content [5]. Therefore, the correction assuming a uniform emissivity value is inappropriate, so estimations are required for each surface type which are highly laborious [2, 4, 5, 23, 26–31]. Techniques for emissivity correction have been summarised by Weng et al. [5, 31].

Table 1. List of commonly measured dependent, independent and intervening variables. *DEP.* Dependent, *IND.* Independent *INT.* Intervening.

Variable	Type	Common indicators		
DEP.	*Climatological*	- Surface temperature (T_{surf})	- Air temperature (T_{air})	- Relative humidity
IND.	*Functional*	- Vegetation indices (*NDVI, EVI*) - Leaf area index (*LAI*)	- Normalised difference water index (*NDWI*)	- Evapotranspiration (ET_o)
	Morphological	- Land-use/land-covers (LULC) - Vegetation, impervious, building and water fractions - Biophysical composition index	- Surface emissivity (ε) - Surface albedo - Soil moisture / soil water content	- Normalised difference built-up index (*NDBI*) - Plant species and type of foliage - Vegetation geometry size and height
	*Configurational (Landscape metrics)**	- Percentage of landscape - Patch area - Patch density - Number of patches - Mean patch size - Mean patch shape index	- Largest patch index - Edge density - Landscape shape index - Mean patch area - Perimeter-area ratio - Aggregation index	- Fractal dimension - Contagion - Shannon's diversity - Area-weighted mean radius of gyration[11] - Local Moran's *I* index
INT.	*Climatological*	- Rainfall and cloud cover - Solar radiation	- Wind direction (V_d) - Wind velocity (V_a)	- Roughness length (Z_o) - Air pressure (P_a)
	Morphological	- Aspect ratio (*H/W*) - Sky view factor (*SVF*)	- Building heights and altitude - Coastal proximity	- Solar orientation/aspect - Anthropogenic heat

*Based on [7, 8, 10, 14, 15, 32, 33] and calculated with FRAGSTATS (McGarigal et al. [34]) and ArcGIS®.

Remotely sensed spectral imagery has been used to identify different land cover fractions and to determine the abundance or amount of vegetation [5, 24, 35]. The number of spectral bands ranges from limited in the case of multispectral imagery (e.g. SPOT and Landsat with 4-8 bands) to very large as hyperspectral data (e.g. AVIRIS with 224 bands). The larger the number of spectral bands, the more the amount of detail and information that can be captured; however, this may increase the costs and time for acquisition, the difficulty of image processing, and the data redundancy between bands [24, 35]. Well-known vegetation indices such as the Normalised Difference Vegetation Index (NDVI) and LAI have been calculated from remotely sensed spectral imagery using software such as ENVI, ERDAS and ArcGIS [24]. Whereas NDVI measures the visible and near-infrared reflectance from vegetation canopy to represent the vigour (healthiness, greenness) of vegetation, LAI provides areal estimations of the total amount of leaves which is related to the interception of solar radiation or shading potential [24, 36]. Both indices serve to calculate the proportion between vegetation and impervious surface fractions and are indicators of ecological function and photosynthetic activity; however, their relationship is nonlinear. The use of vegetation indices raises some issues because they are highly dynamic; depending upon factors such as plant phenology, type of species and methods of estimation (direct and indirect) [36].

LiDAR (light detection and ranging) imagery provides highly accurate three-dimensional information such as terrain elevation, building footprints, and vegetation heights. LiDAR has been used to calculate sky view factors (SVF) or aspect ratios, digital elevation models (DEM), digital surfaces models (DSM), and to extract different vegetation surface fractions (trees, shrubs and low plants) [2, 4, 24, 37–39].

Ground-based monitoring can be implemented to provide auxiliary information and to control the accuracy and precision of remotely sensed imagery [4]; however, only one third of the literature combined in-situ measurements with remote sensing. On-ground monitoring has been mostly conducted using fixed meteorological stations placed at pedestrian levels (1.5 - 2 metres above the ground). These measured air temperature, surface radiant temperature, relative humidity, wind velocity and direction, solar radiation and rainfall. To increase the spatial coverage of in-situ measurements, a few studies employed mobile stations or transects using cars or bicycles [2, 4, 39–42]. This technique requires GPS devices to register the exact time and location to estimate the time lag between measurements over the duration of missions [24]. Experts strongly recommend that ground-based measurements should be deployed simultaneously with data collection from satellites or aircraft to establish better correlations/validations between surface and air temperatures [2, 4, 5, 24].

3.3. Spatial and temporal resolutions

Spatial resolution relates to the level of detail in an image that is defined by the smallest possible feature captured per pixel. Evidence shows that the higher the spatial resolution, the higher the accuracy and precision of results [35]. Three main scales –meso, local and micro– have been identified for climatic studies [43, 44]. The identification of an appropriate scale depends on the extension and type of climatic phenomena to be measured; for instance, meso scale focuses on large urban regions or whole cities, local scale on neighbourhoods and precincts, and micro scale on street canyons and individual structures [44]. Many remotely-sensed projects have been conducted at meso scale and have used freely accessible satellite images of low (AVHRR, MODIS, FY-2C) and medium (Landsat, SPOT and ASTER) spatial resolutions [35] (See Table 2). Despite the advent of very high resolution spaceborne (IKONOS, QuickBird) and airborne imagery (AVIRIS, TASI, HySpex, LiDAR, etc.), less research has been conducted at local and micro scale as the acquisition of this data is costly for most users [2, 4, 35, 45]. However, one of the greatest advantage of airborne remote sensing is the high level of detail [45].

Temporal resolution refers to the amount of time between measurements; an aspect of great importance since vegetation phenology entails functional and structural changes –especially in spring and autumn– that can lead to incorrect estimations [35]. Satellite temporal resolution is defined as the overpass time between two successive images over the same location [35]. Even though spaceborne remote sensing allows time-series analysis, images are occasionally blurred by clouds or poor weather conditions [35]. Extreme temperature and heatwaves conditions mostly occur in summer which has been defined as the preferable season for UHI investigations, and such observations should be conducted at particular times of the day (noon) and night (pre-dawn) [4, 24]. Whereas satellites are constrained in capturing surfaces at optimum times, airborne remote sensing offers a high level of control and flexibility to schedule flights to target specific phenomena [4, 24, 35]. Nevertheless, revisit times are reduced to every 1 to 5 years due to the complex logistics and high costs, which hampers multi-temporal analyses [35]. Conversely, ground-based measurements offer high temporal resolutions, but lack broad spatial coverage [5]. Table 2 summarises the spatial and temporal resolution of common satellite and airborne-based data products.

3.4. Major methods of analysis

The statistical analysis of the relationship between LST and vegetation abundance (NDVI, LAI and fractional surface covers) has been extensively used to analyse the thermal profiles of GI [5]. Evapotranspiration (ET) is another key parameter strongly correlated to vegetation indices that combines the transpiration of plants and evaporation of soils as an indicator of the cooling potential of GI [36]. Nonetheless, the relationship between ET and LST has not been fully investigated because it is difficult to quantify, especially in highly heterogeneous urban settings and at very fine scales [5, 46, 47]. Nouri et al. [46, 47] have reviewed general remote sensing approaches to predict ET from complex vegetated surfaces.

The study of the geometrical and physical properties of urban surfaces and built forms –usually represented by land-use/land-cover (LULC) types– has also served to explain the spatial patterns of LST. Shadows, misclassifications and object occlusion are some of the issues caused when three-dimensional information is derived from two-dimensional imagery that may lead to errors and underestimations [35]. Nevertheless, LiDAR data that focuses on geometrical characteristics can be used in conjunction with spectral imagery for building, surface and vegetation classification and extraction [2, 4, 35]. Weng et al. [5] has noted that simple correlations between LST and LULC are insufficient and that more quantitative and physically-based rather than qualitative descriptors of surfaces should be used in future research. Furthermore, at fine-scales LULC are not able to consider the spatial heterogeneity of vegetated and non-vegetated elements on which thermal cooling depends upon [48–50].

The recent advent of satellite imagery enables calculating spatial autocorrelation indices such as the local Moran's *I* [51] and the FRAGSTATS landscape metrics [34] to examine the role and influence of greenspaces' geometry and distribution on their cooling effects and the spatial patterns of LST. Such effects were analysed by several studies using statistical and predictive models, namely spatial auto-regression, multi-variate linear regression, ANOVA, ordinary least squares (OLS) and Pearson correlation matrix. However, investigations have been mostly conducted at a coarse level and have not fully considered the heterogeneity of greenspaces.

The use of these approaches raises some additional issues as remotely sensed imagery combines the properties, interactions and temperatures of ground surfaces, tree canopy and buildings, and such combinations are nonlinear [5]. Therefore, a three-dimensional analysis of vegetation layers, surfaces and built-up forms is necessary because plants contribute to the modification of temperature, shading, evapotranspiration and air flow differently from soils and buildings [25, 44, 52]. In summary, the integration of thermal, spectral and LiDAR data is strongly recommended for a more comprehensive analysis.

Table 2. Summary of spaceborne and airborne data sources used by reviewed literature.

Data product	Imagery	Acquisition	Spatial resolution	Temporal resolution	# Studies*
Low resolution satellite imagery (>100 m)					
AVHRR	VIS, NIR, SWIR, TIR	Free	1100m	Twice daily	2
MODIS	VIS, NIR, SWIR, TIR	Free	250, 500, 1000m	Daily at 10h30 and 13h30 (local time)	13
FY-2C (FengYun-2)	VIS, TIR, WV	Free	1250, 1440, 5000, 5760m	Every 30 minutes	1
Medium resolution satellite imagery (10-100 m)					
Landsat 5TM	VIS, NIR, SWIR, TIR	Free	30, 120m	Every 16 days at 9h45 (local time)	21
Landsat 7ETM+	VIS, NIR, SWIR, TIR	Free	15, 30, 60m	Every 16 days at 10h00 (local time)	15
Landsat 8	VIS, NIR, SWIR, TIR, PAN	Free	15, 30, 60, 100 m	Every 16 days at 10h00 (local time)	2
SPOT	VIS, NIR, SWIR, PAN	Purchased	2.5, 10, 20m	Every 1-3 days	3
ASTER	VIS, NIR, SWIR, TIR	Free & purchased	15, 30, 90m	Daily at 10h30 (local time)	8
High resolution satellite imagery (<10 m)					
IKONOS	VIS, NIR, PAN	Purchased	0.8, 4m	Every 3 days	6
World-View 2	NIR, TIR, PAN	Purchased	0.5, 1.8, 2.4 m	Every 1-2 days	1
QuickBird	VIS, NIR, PAN	Purchased	0.6, 2.4, 2.6 m	Every 2-6 days at 10h30 (local time) & on demand	7
Airborne imagery (resolutions depending on sensors)					
MASTER	VIS, NIR, SWIR, TIR	Purchased	7m, 50 m	On demand	2
AVIRIS	VIS, NIR, SWIR	Purchased	4 m, 20 m	On demand	1
TASI	TIR	Purchased	0.6 m, 1.25 m	On demand	1
SASI	SWIR	Purchased	1.25 m	On demand	1
DAMS	TIR, NIR, UV	Purchased	5 m	On demand	1
HySpex	VIS, NIR	Purchased	0.5 m, < 1m	On demand	2
Infratec	TIR	Purchased	0.7 m	On demand	1
FLIR	TIR	Purchased	0.5 m	On demand	2

Adapted from Irger[24] & Weng [35]. *NIR* Near infrared, *PAN* Panchromatic, *SWIR* Short-wave infrared, *TIR* Thermal infrared, *UV* Ultraviolet, *VIS* Visible light, *WV* Water vapor. ** Sone studies used more than one data product at a time.*

4. Developing a new methodological framework

4.1. Data sources and calculation of variables

Based on the reviewed literature, we recommend the combination of airborne remote sensing and ground measurements to collect the relevant information necessary for the thermal evaluation of GI at local and micro scale. Figure 1 presents a schematic overview of the most essential dependent, independent and intervening variables (as per Table 1) and how these can be derived from data sources.

Among all variables the estimation of evapotranspiration (ET) in urban contexts remains unexplored since most research has been conducted in homogeneous environments, particularly in agricultural studies. Also, ET estimations are challenging due to the highly diverse conditions of plant species, canopy covers, microclimates, and the presence of impervious surfaces [46]. For the present framework, we will incorporate Nouri et al. [53, 54] remote sensing approach –based on the FAO-56 Penman-Monteith method [55]– to quantify daily ET using vegetation indices (NDVI/EVI) derived from spectral imagery and reference ET obtained from meteorological data (either mobile or fixed stations) (See Figure 1).

The calculation of configurational parameters will serve to determine the level of aggregation or clumpiness of vegetation features (especially trees). These landscape metrics can be calculated once vegetation features have been extracted from LiDAR data and validated against NDVI values (See Figure 1).

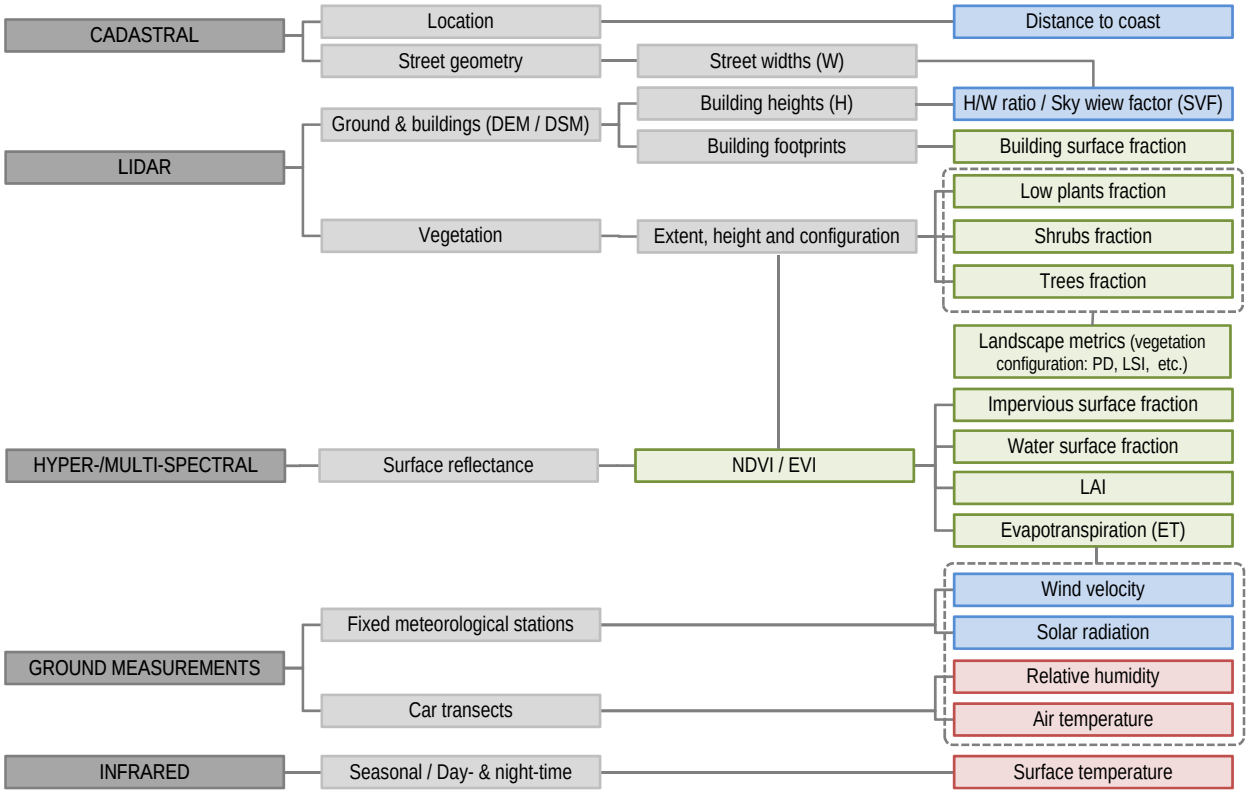

Fig. 1. Schematic overview of essential dependent (red colour), independent (green colour) and intervening (blue colour) variables derived from their corresponding data sources (dark grey). (Based on Irger [24]).

4.2. Data acquisition protocols

Following a review of studies [2, 4, 24], we propose a set of specifications for data acquisition that can be applied irrespective of geographic locations; even so, flight protocols depend on several temporal and meteorological considerations. Most severe UHIs are likely to happen during summer after several days of continuous heatwave; however, such warming conditions may be more desirable in winter [24]. The best time to study the thermal profiles of vegetation and SUHIs is during the day, especially around noon giving the high angle and intensity of the sun which enables capturing the maximum surface temperatures with minimal shading effects. Contrastingly, UHIs within the urban canopy layer are usually more pronounced at night-time, especially in the early morning (pre-dawn) when surfaces have lost the maximum amount of radiative energy and the urban-rural thermal differences are greatest [2, 4, 24]. Also, surface to air temperature correlations are stronger at night giving the lack of building shade and traffic flows contributing to the anthropogenic heat [4].

To investigate the capacity of GI to mitigate excess heat, flights should preferably be undertaken during periods of two to three consecutive hot days and missions should be brief (<60 minutes) to avoid large temperature differences between locations [2, 4]. Nevertheless, some degree of flexibility when allocating the flight times and duration is needed to reduce the risk of missing suitable opportunities. The acquisition of LiDAR data can be carried out either simultaneously or separately from the TIR and spectral imagery; however, this must correspond to the same period/season to prevent changes caused by the vegetation phenology.

Successful data collection requires suitable meteorological conditions. Clear skies are essential since cloud cover may obstruct the aircraft's sensors. Cloudy skies hinder capturing accurate thermal imagery by irregularly shading the ground at daytime, and preventing long-wave radiative cooling at night-time. Similarly, low wind speeds are preferable as high velocities increase surface cooling effects, reduce atmospheric stability, and cause air turbulence [4, 24, 56], affecting the accuracy of thermal data and preventing optimal correlations between air and surface temperatures. Another crucial factor is that study areas must not have experienced any precipitation three to five days prior to the flights as this can alter ET estimations and distort surface temperatures.

The type of sensors and altitude of flights are important to determine the spatial resolution of imagery that will depend on the type of analysis. We recommend to use very high resolution imagery (<2m) for the thermal analysis of GI at local and micro scales. Additionally, airborne-based measurements can be complemented by concurrent ground-based monitoring [2, 4]. Mobile transects can be used to obtain a good spatial coverage of canopy layer conditions and should include a GPS tracker, meanwhile fixed meteorological stations can be used if higher temporal resolutions are required. In both cases, devices must be placed between one to two metres above the ground.

4.3. Workflow and implementation

In this section we present a GIS-based workflow for the implementation of our methodological framework (Figure 2) that draws on a method developed by Irger [24]. It is necessary to recognise the critical influence that intervening variables have on the thermal performance of GI and the variability of UHIs. Hence, measurements must be conducted in calm, clear and dry conditions to reduce the moderating effects of wind (especially sea breezes), cloud cover and rainfall.

An appropriate classification of urban form is also necessary for a meaningful comparison of GI typologies by taking into account the spatial and structural disparities of urban landscapes. We recommend to apply the LCZs proposed by Stewart and Oke [49, 52], a standardised scheme specifically intended to classify observation sites for UHI studies based on climate-relevant surface properties. Protocols for automated classification of LCZs using remote sensing data have been applied by the World Urban Database and Access Portal Tools (WUDAPT) initiative [57–59] and several studies [24, 60–63]. However, further work is still needed to improve the accuracy of classifications and to integrate three-dimensional auxiliary data such as LiDAR. Furthermore, research has demonstrated that the use of grid cells with 100 metres of spacing provide optimal results for morphological classifications without compromising the amount of detail or causing landscape fragmentation [24, 57].

Previous research has introduced a new GI typology to support urban microclimate studies [25, 50] that is incorporated into this framework for the classification of GI according to functional, structural and configurational attributes. To enable a more comprehensive and finer analysis of GI, LCZs must be sub-divided into grids of 50 metres of length and width and subsequently classified into corresponding typologies. Then, all the independent variables (e.g. NDVI, LAI and ET) summarised in Figure 1 have to be quantified and assigned to each cell by calculating their mean values.

The last step involves the computation of LST that should be corrected with spectral emissivity values as described in section 3.2 and validated against ground-based air temperatures. Mean LST values have to be assigned to each GI typology for subsequent spatial and statistical correlation between variables, and for the elaboration of predictive numerical models using any of the methods mentioned in section 3.4. The schematic representation of the proposed framework with a list of relevant data sources and variables are presented in Figure 2.

5. Conclusions

Remote sensing methods have mostly focused on mapping and quantifying the cooling effects of GI at meso scales using satellite imagery; however, further research at local and micro scales is still required. To respond to this gap, this paper overviews recent literature and presents a methodological framework for a more precise and accurate evaluation of the thermal profiles of different GI typologies using a combination of airborne remote sensing and ground-monitoring. The proposed framework includes the following steps: (a) the control of intervening variables

and the moderating effects of urban morphology through the classification of sites using the LCZ scheme; (b) the sub-classification of LCZs into a newly developed GI typology and subsequent estimation of functional indicators (NDVI, LAI and ET), structural indicators (surface cover fractions) and landscape metrics; and (c) the statistical correlations between GI-derived variables and LST to predict particular microclimatic outcomes from each typology. This is a preliminary methodology that remains provisional since it is part of an ongoing research. Further stages will concentrate on developing specific GIS-based workflows for testing and validating it using Sydney and Melbourne as case studies.

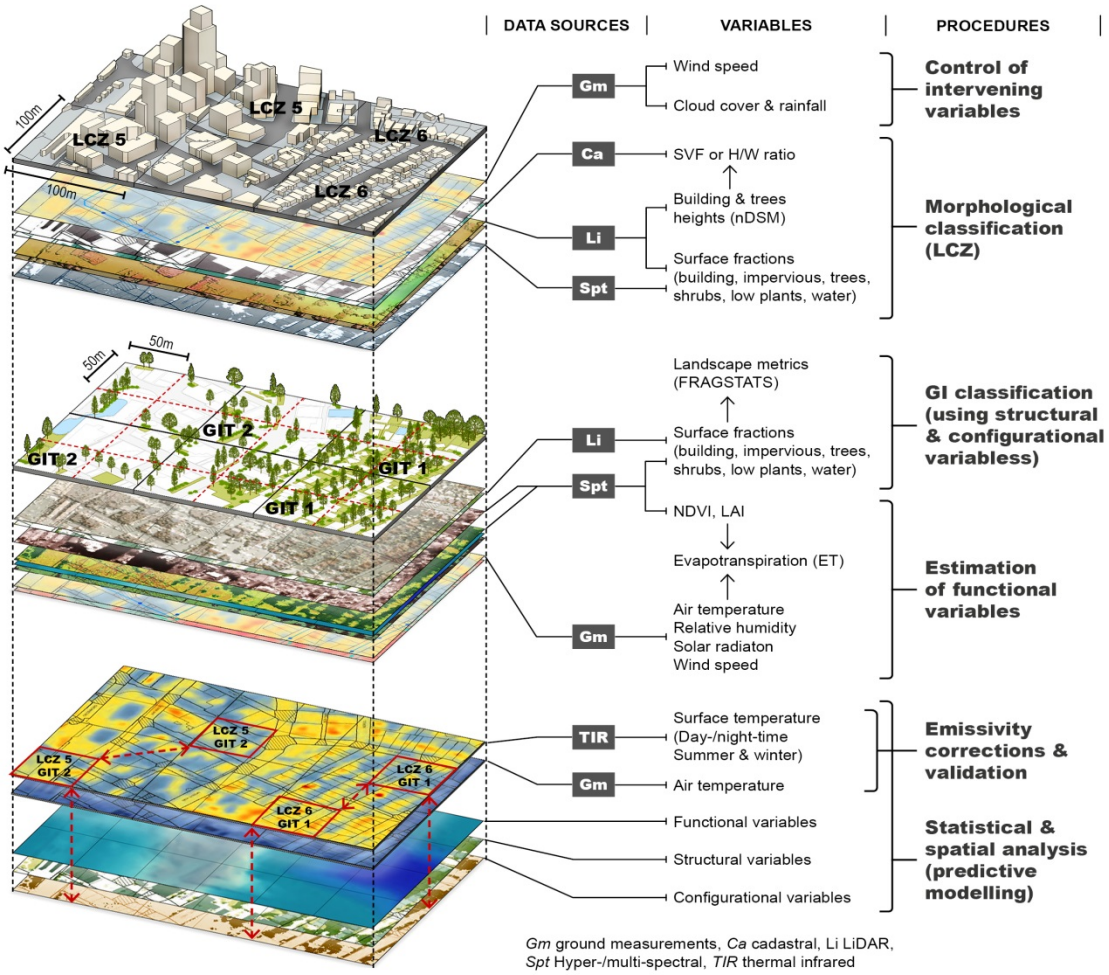

Fig. 2. Schematic representation of the methodological framework and list of relevant data sources and variables.

Acknowledgements

This paper is possible thanks to the financial support provided by the Faculty of Built Environment, University of New South Wales (UNSW-Australia) and the Cooperative Research Centre for Low Carbon Living (CRC-LCL).

References

[1] Huang, L., Shen, H., Wu, P., Zhang, L., and Zeng, C., Eds. *Relationships analysis of land surface temperature with vegetation indicators and impervious surface fraction by fusing multi-temporal and multi-sensor remotely sensed data*. 2015.

[2] Coutts, A. M., Harris, R. J., Phan, T., Livesley, S. J., Williams, N., and Tapper, N. J. Thermal infrared remote sensing of urban heat. hotspots, vegetation, and an assessment of techniques for use in urban planning. *Remote Sensing of Environment*. 2016.
[3] Hou, P., Jiang, W., Cao, G., and Luo, A., Eds. *Effect of urban thermal characteristics on wetlands based on remote sensing and GIS*. 2009.
[4] Harris, R. J. and Coutts, A. M. *Airborne Thermal Remote Sensing for Analysis of the Urban Heat Island*. Victorian Centre for Climate Change Adaptation Research (VCCCAR), Melbourne, Australia. 2011.
[5] Weng, Q. Thermal infrared remote sensing for urban climate and environmental studies. Methods, applications, and trends. *ISPRS Journal of Photogrammetry and Remote Sensing*. 2009; 64,4:335–44.
[6] Fan, C., Myint, S. W., and Zheng, B. Measuring the spatial arrangement of urban vegetation and its impacts on seasonal surface temperatures. *Progress in Physical Geography*. 2015; 39,2:199–219.
[7] Maimaitiyiming, M., Ghulam, A., Tiyip, T., Pla, F., Latorre-Carmona, P., Halik, Ü., Sawut, M., and Caetano, M. Effects of green space spatial pattern on land surface temperature. Implications for sustainable urban planning and climate change adaptation. *ISPRS Journal of Photogrammetry and Remote Sensing*. 2014; 89:59–66.
[8] Li, X., Zhou, W., and Ouyang, Z. Relationship between land surface temperature and spatial pattern of greenspace. What are the effects of spatial resolution? *Landscape and Urban Planning*. 2013; 114:1–8.
[9] Li, X., Zhou, W., Ouyang, Z., Xu, W., and Zheng, H. Spatial pattern of greenspace affects land surface temperature. Evidence from the heavily urbanized Beijing metropolitan area, China. *Landscape Ecol*. 2012; 27,6:887–98.
[10] Zhou, W., Huang, G., and Cadenasso, M. L. Does spatial configuration matter? Understanding the effects of land cover pattern on land surface temperature in urban landscapes. *Landscape and Urban Planning*. 2011; 102,1:54–63.
[11] Xiao, R.-b., Ouyang, Z., Zheng, H., Li, W.-f., Schienke, E. W., and WANG, X.-k. Spatial pattern of impervious surfaces and their impacts on land surface temperature in Beijing, China. *Journal of Environmental Sciences*. 2007; 19,2:250–6.
[12] Wu, J., Jenerette, G. D., Buyantuyev, A., and Redman, C. L. Quantifying spatiotemporal patterns of urbanization. The case of the two fastest growing metropolitan regions in the United States. *Ecological Complexity*. 2011; 8,1:1–8.
[13] Rasul, A., Balzter, H., and Smith, C. Spatial variation of the daytime Surface Urban Cool Island during the dry season in Erbil, Iraqi Kurdistan, from Landsat 8. *Urban Climate*. 2015; 14:176–86.
[14] Chen, A., Yao, X. A., Sun, R., and Chen, L. Effect of urban green patterns on surface urban cool islands and its seasonal variations. *Urban Forestry & Urban Greening*. 2014; 13,4:646–54.
[15] Kong, F., Yin, H., James, P., Hutyra, L. R., and He, H. S. Effects of spatial pattern of greenspace on urban cooling in a large metropolitan area of eastern China. *Landscape and Urban Planning*. 2014; 128:35–47.
[16] Tan, M. and Li, X. Integrated assessment of the cool island intensity of green spaces in the mega city of Beijing. *International Journal of Remote Sensing*. 2013; 34,8:3028–43.
[17] Sun, R., Chen, A., Chen, L., and Lü, Y. Cooling effects of wetlands in an urban region. The case of Beijing. *Ecological Indicators*. 2012; 20:57–64.
[18] Cheng, X., Wei, B., Chen, G., Li, J., and Song, C. Influence of Park Size and Its Surrounding Urban Landscape Patterns on the Park Cooling Effect. *J. Urban Plann. Dev.* 2014.
[19] Feyisa, G. L., Dons, K., and Meilby, H. Efficiency of parks in mitigating urban heat island effect. An example from Addis Ababa. *Landscape and Urban Planning*. 2014; 123:87–95.
[20] Kong, F., Yin, H., Wang, C., Cavan, G., and James, P. A satellite image-based analysis of factors contributing to the green-space cool island intensity on a city scale. *Urban Forestry & Urban Greening*. 2014; 13,4:846–53.
[21] Cao, X., Onishi, A., Chen, J., and Imura, H. Quantifying the cool island intensity of urban parks using ASTER and IKONOS data. *Landscape and Urban Planning*. 2010; 96,4:224–31.
[22] Bowler, D. E., Buyung-Ali, L., Knight, T. M., and Pullin, A. S. Urban greening to cool towns and cities: A systematic review of the empirical evidence. *Landscape and Urban Planning*. 2010; 97,3:147–55.
[23] Coutts, A. M. and Harris, R. J. *A multi-scale assessment of urban heating in Melbourne during an extreme heat event. policy approaches for adaptation*. Victorian Centre for Climate Change Adaptation Research (VCCCAR), Melbourne, Australia. 2012.
[24] Irger, M. *The Effect of Urban Form on Urban Microclimate*. PhD Thesis, Faculty of Built Environment, The University of New South Wales. 2014.
[25] Bartesaghi Koc, C., Osmond, P., and Peters, A., Eds. *A green infrastructure typology matrix to support urban microclimate studies*, Singapore. 2016.
[26] Jenerette, G. D., Harlan, S. L., Buyantuev, A., Stefanov, W. L., Declet-Barreto, J., Ruddell, B. L., Myint, S. W., Kaplan, S., and Li, X. Micro-scale urban surface temperatures are related to land-cover features and residential heat related health impacts in Phoenix, AZ USA. *Landscape Ecol*. 2015.
[27] Gee, O. K. and Sarker, M. L. R. Monitoring the effects of land use/landcover changes on urban heat island. In *SPIE Remote Sensing*. SPIE Proceedings. SPIE:889304. 2013. DOI=10.1117/12.2029035.
[28] Qiao, Z., Tian, G., and Xiao, L. Diurnal and seasonal impacts of urbanization on the urban thermal environment. A case study of Beijing using MODIS data. *ISPRS Journal of Photogrammetry and Remote Sensing*. 2013; 85:93–101.
[29] Zhou, J., Chen, Y., Zhang, X., and Zhan, W. Modelling the diurnal variations of urban heat islands with multi-source satellite data. *International Journal of Remote Sensing*. 2013; 34,21:7568–88.
[30] Xiao, K. and Xu, H., Eds. *RS and GIS-based Analysis of Urban Heat Island Effect in Shanghai*. 2010.
[31] Weng, Q., Lu, D., and Schubring, J. Estimation of land surface temperature–vegetation abundance relationship for urban heat island studies. *Remote Sensing of Environment*. 2004; 89,4:467–83.

[32] Connors, J. P., Galletti, C. S., and Chow, W. T. L. Landscape configuration and urban heat island effects. Assessing the relationship between landscape characteristics and land surface temperature in Phoenix, Arizona. *Landscape Ecol*. 2013; 28,2:271–83.
[33] Kong, F. and Nakagoshi, N. Spatial-temporal gradient analysis of urban green spaces in Jinan, China. *Landscape and Urban Planning*. 2006; 78,3:147–64.
[34] McGarigal, K., Cushman, S.A., Neel, M.C., Ene, E. *FRAGSTATS. Spatial Pattern Analysis Program for Categorical Maps*. University of Massachusetts, Amherst (www.umass.edu/landeco/research/fragstats/fragstats.html). 2002.
[35] Weng, Q. Remote sensing of impervious surfaces in the urban areas. Requirements, methods, and trends. *Remote Sensing of Environment*. 2012; 117:34–49.
[36] Hunter, A., Livesley, S. J., and Williams, N. S. G. *Literature Review. Responding to the Urban Heat Island: A Review of the Potential of Green Infrastructure*. Report funded by the Victorian Centre for Climate Change Adaptation (VCCCAR). Victorian Centre for Climate Change Adaptation (VCCCAR), Melbourne, Australia. 2012.
[37] Emmanuel, R. and Loconsole, A. Green infrastructure as an adaptation approach to tackling urban overheating in the Glasgow Clyde Valley Region, UK. *Landscape and Urban Planning*. 2015; 138:71–86.
[38] Konarska, J., Holmer, B., Lindberg, F., and Thorsson, S. Influence of vegetation and building geometry on the spatial variations of air temperature and cooling rates in a high-latitude city. *Int. J. Climatol.* 2015:n/a-n/a.
[39] Su, W., Zhang, Y., Yang, Y., and Ye, G. Examining the Impact of Greenspace Patterns on Land Surface Temperature by Coupling LiDAR Data with a CFD Model. *Sustainability*. 2014; 6,10:6799–814.
[40] Heusinkveld, B. G., Steeneveld, G. J., van Hove, L. W. A., Jacobs, C. M. J., and Holtslag, A. A. M. Spatial variability of the Rotterdam urban heat island as influenced by urban land use. *J. Geophys. Res. Atmos.* 2014; 119,2:677–92.
[41] Bilgili, B. C., Şahin, Ş., Yilmaz, O., Gürbüz, F., and Arici, Y. K. Temperature distribution and the cooling effects on three urban parks in Ankara, Turkey. *IJGW*. 2013; 5,3:296.
[42] Schwarz, N., Schlink, U., Franck, U., and Großmann, K. Relationship of land surface and air temperatures and its implications for quantifying urban heat island indicators—An application for the city of Leipzig (Germany). *Ecological Indicators*. 2012; 18:693–704.
[43] Oke, T. R. Towards better scientific communication in urban climate. *Theor. Appl. Climatol.* 2006; 84,1-3:179–90.
[44] Erell, E., Pearlmutter, D., and Williamson, T. *Urban Microclimate. Designing the Spaces Between Buildings*. Earthscan, London, Washington, DC. 2011.
[45] Liu, K., Su, H., Zhang, L., Yang, H., Zhang, R., and Li, X. Analysis of the Urban Heat Island Effect in Shijiazhuang, China Using Satellite and Airborne Data. *Remote Sensing*. 2015; 7,4:4804–33.
[46] Nouri, H., Beecham, S., Anderson, S., Hassanli, A. M., and Kazemi, F. Remote sensing techniques for predicting evapotranspiration from mixed vegetated surfaces. *Urban Water Journal*. 2015; 12,5:380–93.
[47] Nouri, H., Beecham, S., Kazemi, F., and Hassanli, A. M. A review of ET measurement techniques for estimating the water requirements of urban landscape vegetation. *Urban Water Journal*. 2013; 10,4:247–59.
[48] Cadenasso, M. L., Pickett, S. T. A., McGrath, B., and Marshall, V. Ecological Heterogeneity in Urban Ecosystems. Reconceptualized Land Cover Models as a Bridge to Urban Design. In *Resilience in Ecology and Urban Design. Linking Theory and Practice for Sustainable Cities*, S. Pickett, M. L. Cadenasso and B. McGrath, Eds. Springer, New York. 2013.
[49] Stewart, I. D. and Oke, T. R. Local Climate Zones for Urban Temperature Studies. *Bull. Amer. Meteor. Soc.* 2012; 93,12:1879–900.
[50] Bartesaghi Koc, C., Osmond, P., and Peters, A. Towards a comprehensive green infrastructure typology. A systematic review of approaches, methods and typologies. *Urban Ecosyst*. 2016.
[51] Anselin, L. Local Indicators of Spatial Association - LISA. *Geographical Analysis*. 1995; 27,2:93–115.
[52] Stewart, I. D. *Redefining the Urban Heat Island*. Doctor of Philosophy - PhD, University of British Columbia. 2011.
[53] Nouri, H., Glenn, E., Beecham, S., Chavoshi Boroujeni, S., Sutton, P., Alaghmand, S., Noori, B., and Nagler, P. Comparing Three Approaches of Evapotranspiration Estimation in Mixed Urban Vegetation. Field-Based, Remote Sensing-Based and Observational-Based Methods. *Remote Sensing*. 2016; 8,6:492.
[54] Nouri, H., Beecham, S., Anderson, S., and Nagler, P. High Spatial Resolution WorldView-2 Imagery for Mapping NDVI and Its Relationship to Temporal Urban Landscape Evapotranspiration Factors. *Remote Sensing*. 2014; 6,1:580–602.
[55] Allen, R. G., Pereira, L. S., Raes, D., and Smith, M. *Crop evapotranspiration - Guidelines for computing crop water requirements - FAO Irrigation and drainage paper 56*. Food and Agriculture Organization of the United Nations (FAO), Rome. 1998.
[56] Oke, T. R. *Boundary Layer Climates*. Routledge, London [England], New York. 1992.
[57] Bechtel, B., Alexander, P., Böhner, J., Ching, J., Conrad, O., Feddema, J., Mills, G., See, L., and Stewart, I. Mapping Local Climate Zones for a Worldwide Database of the Form and Function of Cities. *IJGI*. 2015; 4,1:199–219.
[58] Kaloustian, N. and Bechtel, B., Eds. *Local Climatic Zoning and Urban Heat Island in Beirut*. NUS, Singapore. 2016.
[59] Ren, C., Cai, M., Wang, R., Xu, Y., and Ng, E., Eds. *Local Climate Zone (LCZ) Classification Using the World Urban Database and Access Portal Tools (WUDAPT) Method: A Case Study in Wuhan and Hangzhou*. NUS, Singapore. 2016.
[60] Bechtel, B. and Daneke, C. Classification of Local Climate Zones Based on Multiple Earth Observation Data. *IEEE J. Sel. Top. Appl. Earth Observations Remote Sensing*. 2012; 5,4:1191–202.
[61] Kotharkar, R. and Bagade, A., Eds. *Local Climate Zone Classification for Indian Cities: A Case study of Nagpur*. NUS, Singapore. 2016.
[62] Kotharkar, R., Bagade, A., and Kandya, A., Eds. *Study of Urban Heat Island Effect using Local Climate Zone and Land Surface Temperature using Landsat 7 ETM+ for Nagpur, India.* NUS, Singapore. 2016.
[63] Zheng, Y., Ren, C., Wang, R., Ho, J., Lau, K., and Ng, E., Eds. *GIS-based Mapping of Local Climate Zone in the High-density City of Hong Kong*, Singapore. 2016.